



# Effect of weld metal ferrite content on mechanical properties and stress corrosion cracking resistance in 22 Cr 5 Ni duplex stainless steel

P. K. Nanavati<sup>1</sup> · D. J. Kotecki<sup>2</sup> · Sanjay N. Soman<sup>3</sup>

Received: 12 November 2018 / Accepted: 30 January 2019 / Published online: 13 February 2019  
© International Institute of Welding 2019

## Abstract

Welded 22 Cr 5 Ni duplex stainless steel is often used for chloride-containing environments and sour service applications. Chloride stress corrosion cracking (CSCC) during service poses a threat to the service life of the weldment. Yield strength and resistance to CSCC are considered to depend on the weld metal ferrite content, which is variously required to be 30 to 60%, 30 to 70 ferrite number, 35 to 75%, etc. Accordingly, the present work has been carried out in collaboration with a filler metal manufacturer to investigate the research gap pertaining to minimum ferrite content to obtain the required minimum weld metal yield strength and resistance to CSCC. In this study, 22 Cr 5 Ni weldments with weld metal ferrite content in the range of 14% to 30%, or 20 to 40 ferrite number, obtained by increasing the filler metal nickel content above the normal 9%, have been prepared and investigated. It was found that yield strength and tensile strength requirements of base metal and filler metal classifications were exceeded at all ferrite levels investigated and that no CSCC was observed after 1000-h exposure in the ASTM G 123 boiling 25% sodium chloride test.

**Keywords** Duplex stainless steel · Shielded metal arc welding · Ferrite content · Ferrite number · Chloride stress corrosion cracking · Weld metal yield strength

## 1 Introduction

Duplex stainless steels (DSSs) are promising candidate materials, finding increasing use in the process industries and are being widely employed in various industries, such as petrochemical plants, off-shore platforms, oil and gas, paper and

pulp. DSSs offer an economical combination of mechanical strength (twice the yield strength of austenitic stainless steels) coupled with excellent corrosion/stress corrosion cracking resistance compared with austenitic stainless steels and better formability and lower transition temperature than ferritic stainless steels [1–6].

DSSs typically have an annealed structure of approximately equal amounts of ferrite and austenite, although the ratios can vary from approximately 35/65 to 55/45 in wrought steel. Most applications, where DSSs are used, are aggressive, and DSSs or other higher alloys are required for adequate corrosion resistance [1].

Duplex stainless steels have far-reaching, successful service records in corrosive and erosive environments up to 315 °C (600 °F), while providing high immunity to chloride stress corrosion cracking (CSCC) [2]. DSSs are often used in lieu of austenitic stainless steels in services where the common austenitic stainless steel would have problems with pitting or CSCC [2].

Most of the industrial components made of these DSSs are fabricated primarily by welding using almost all the conventional welding processes including shielded metal arc welding (SMAW), gas metal arc welding (GMAW), gas tungsten arc

---

Recommended for publication by Commission II - Arc Welding and Filler Metals

---

✉ P. K. Nanavati  
pknanavati@gecg28.ac.in

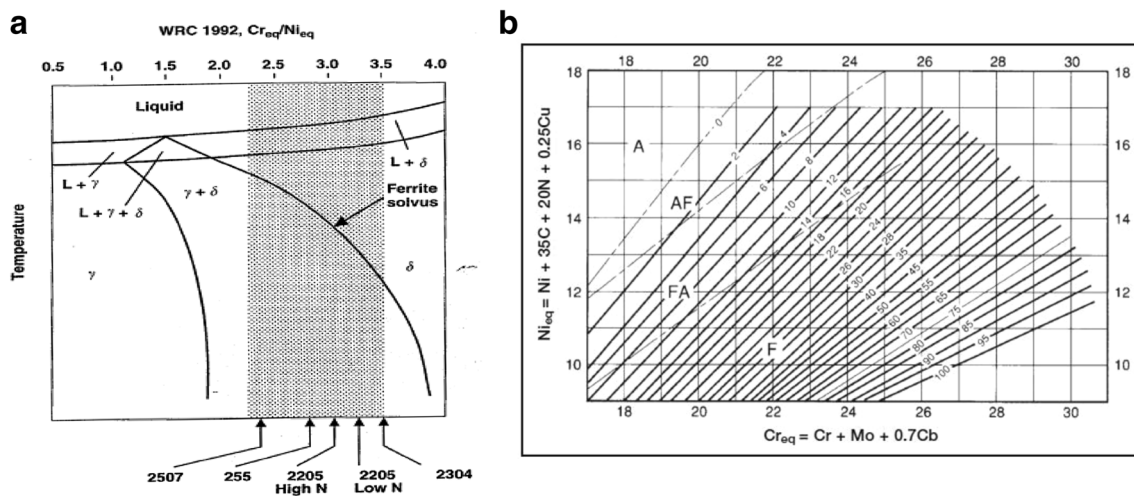
D. J. Kotecki  
damian@damiankotecki.com

Sanjay N. Soman  
somansn@yahoo.com

<sup>1</sup> Metallurgy Department, Government Engineering College, Sec-28, Gandhinagar, Gujarat, India

<sup>2</sup> Damian Kotecki Welding Consultants, Inc., Chapel Hill, NC, USA

<sup>3</sup> Metallurgical and Materials Engineering department, Faculty of Technology and Engineering, The M. S. University of Baroda, Vadodara, Gujarat, India



**Fig. 1** a Elevated temperature region of a pseudo binary phase diagram for DSS. Shaded region represents the range for commercial alloys. Source: [5]. b WRC-1992 diagram including solidification mode boundaries. Source: [15]

welding (GTAW), submerged arc welding (SAW), and flux cored arc welding (FCAW) [3].

Among industrial clients, there has been a dispute over the issue of required minimum ferrite content. The issue generally does not involve GTAW or GMAW because the low oxygen content (typically less than 150 ppm) of the weld metal provides high toughness at relatively high ferrite content, so filler metal manufacturers can aim for about 50% ferrite in their filler metal without concern about toughness. But for flux shielded filler metals (SMAW, FCAW, SAW), the higher oxygen content (typically 400 ppm or more) reduces toughness, so the filler metal manufacturer aims for weld metal deposits at the low end of specified ferrite ranges in order to meet toughness requirements at  $-40\text{ }^{\circ}\text{C}$ . There is, of course, a degree of variation in weld metal ferrite content and in reproducibility of measurement. As a result, it happens fairly often that a fabricator measures, in flux shielded filler metal, a little less than the specified ferrite requirement or the fabricator measures above the specified limit but his customer measures ferrite content for the same lot of filler metal and obtains a value below the specified limit. Then there is a dispute over whether or not the filler metal is acceptable, and a delay in the project takes place while the parties in the dispute try to resolve it. This wastes a lot of time and money.

There are two main concerns about the minimum ferrite content requirement for DSSs: maintaining required minimum yield strength and providing resistance to CSCC [4].

A few notable research studies have been taken place on finding a relationship between DSS ferrite content and mechanical strength and/or CSCC resistance. CSCC through

constant-extension-rate (CER) tensile test method was examined by Baeslack et al. [7] in 304-L weldments made by pulsed GMAW with varying weld metal ferrite number (FN) of 0, 1, 4, 6, 11, and 22 using ER310 or ER312 filler metal followed by autogenous GTAW fusion with the base metal. A continuous ferrite network at 22 FN was found to improve ductility under CSCC testing.

Kotecki [4] experimented on alloys 2205 and 255 in the as-welded condition, using self-shielded FCAW electrodes of 5.5% to over 10% nickel. He found that weld deposit below 60 FN for alloy 2205 and 255 provides sufficient ductility to pass a 2-T bend test, Charpy V-notch energy of better than 20 ft-lb (27 J) at  $-50\text{ }^{\circ}\text{F}$  ( $-46\text{ }^{\circ}\text{C}$ ). Ferrite content above 30 FN (approximately 21%) results in yield strength and tensile strength in the weld metal exceeding base metal requirements. Ferrite content above about 70 FN (about 50%) resulted in low weld metal ductility and toughness. No ferrite level below 30FN was investigated, and CSCC behavior was not investigated.

The studies on CSCC of DSS in  $\text{H}_2\text{S}/\text{CO}_2$  and Cl-environments conducted by Van Gelder et al. [8] revealed that at higher temperature DSS is susceptible to CSCC when subjected to slow plastic strain rate.

Krishnan et al. [9] studied CSCC behavior of austenitic stainless steel weld metals with varying ferrite contents produced using the SAW strip cladding process coupled with GTAW, subsequently post weld heat treated for varying temperatures and times. The results showed that a discontinuous ferrite network is more beneficial for resistance to CSCC than a continuous network, opposite to the findings of Baeslack

**Table 1** Chemical composition of 2205 plates

C	Si	Mn	P	S	Cr	Ni	Mo	Nb	Cu	Co	N
0.023	0.37	1.50	0.018	0.001	22.37	5.72	3.21	0.11	0.14	0.08	0.177

**Table 2** Chemical composition of electrode deposits as provided by the supplier

SMAW electrode deposit with target Ni content	C	Mn	Si	S	P	Cr	Ni	Mo	Cu	N
Standard E2209-16 (9% Ni)	0.031	1.08	0.59	0.007	0.025	22.38	9.20	3.35	0.096	0.18
A electrode (9.5–10.5% wt.)	0.019	0.99	0.61	0.005	0.027	22.29	9.8	3.19	0.068	0.17
B electrode Ni (10.5–11.5% wt.)	0.021	0.99	0.58	0.007	0.028	22.35	10.80	3.16	0.075	0.16
C electrode (11.5–12.5% wt.)	0.017	1.11	0.62	0.008	0.028	22.33	12.55	3.20	0.069	0.18

et al. [4]. Welds deposited by the low heat input GTAW process showed better CSCC resistance than their SAW counterparts because they had a finer ferrite network. The overall cracking was due to CSCC in austenite and anodic dissolution of ferrite. The CSCC tests were conducted on notched tensile samples in a 5 M H<sub>2</sub>SO<sub>4</sub> + 0.5 M NaCl solution at room temperature.

Widmanstatten austenite (WA), intergranular austenite (IGA), and partially transformed austenite (PTA) in the HAZ were found by Liou et al. [10] to have a beneficial effect on CSCC resistance. However, grain boundary austenite was found to promote the occurrence of intergranular CSCC in CaCl<sub>2</sub> solution at 100 °C.

Raman et al. [11] found that nitrogen additions up to 2800 ppm to super duplex UNS S32750 grade improved CSCC resistance, but beyond 5600 ppm nitrogen, CSCC susceptibility increases.

Studies of CSCC in UNS S31603 and UNS S32750 wrought samples and electrochemical analysis pitting measurement conducted by Aljoboury et al. [12] provided recommendations for building brine recirculation pumps. UNS S32750 samples showed superior stress corrosion cracking resistance compared with that of UNS S31603 material in the same testing conditions.

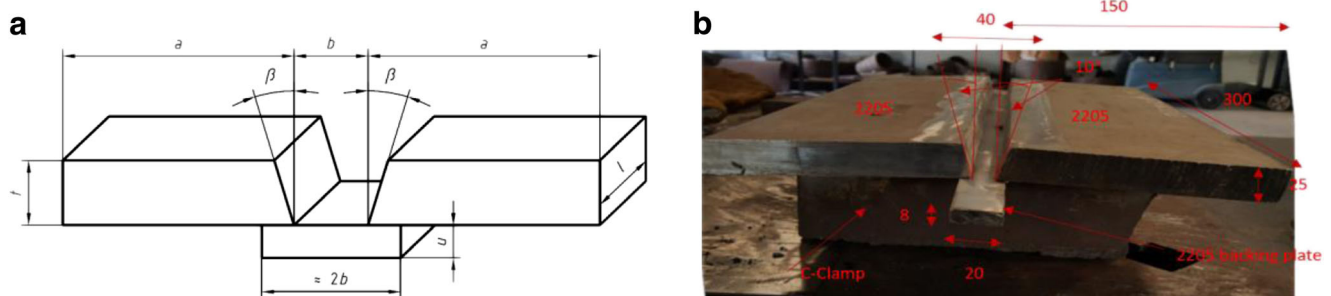
Study of weld failure in a 2205 duplex stainless steel nozzle conducted by Yang et al. [13] revealed a root cause that localized uneven distribution of ferrite/austenite with 80–90% ferrite in weld metal as responsible for the cleavage fracture along columnar grains.

Potgieter et al. [14] examined the influence of nickel additions (5%, 7%, 9%, and 13%) on the pitting corrosion behavior of low nitrogen 22% Cr DSS. Their results showed that uniform corrosion behavior of the alloys was predominantly controlled by phase composition and ratio while pitting resistance is controlled by nickel content.

These studies show a considerable research gap to understanding the relationship among ferrite content, mechanical strength, and CSCC susceptibility of duplex stainless steel welds. The literature survey finds that there has been a lack of data to support a minimum ferrite content requirement for DSS weld metal to meet the requirement of minimum yield strength and resistance to CSCC [1–14].

From a metallurgical point of view, DSS generally requires solidification as essentially 100% ferrite, followed by formation of austenite only in the solid state. This solidification mode, as depicted in Fig. 1a, is considered to be responsible for both high yield strength and resistance to CSCC. The WRC-1992 diagram (Fig. 1b) indicates 100% ferrite solidification at as low as 20 ferrite number (about 14% ferrite).

Accordingly, the present work has been carried out to examine the required minimum ferrite content to obtain required minimum yield strength and resistance to CSCC. Under this project, filler metal was provided in the form of covered electrodes of varied nickel content. Nickel contents of nominally 9.5–10.5% (within the 8.5–10.5% Ni range for E2209 covered electrodes of AWS A5.4, but not normally produced commercially due to concern about low ferrite), 10.5 to 11.5%, and 11.5 to 12.5% by weight were targeted, with other elements



**Fig. 2** a Schematic of weld test setup [16]. b Actual weld test setup before welding

**Table 3** Joint dimensions, mm except where noted

Type	<i>T</i>	<i>a</i>	<i>b</i>	<i>u</i>	$\beta$ , degree	<i>L</i>
1.4	25	$\geq 150$	20	$\geq 6$	$10_0^{+2.5}$	$\geq 150$

held constant. This is in comparison to normal commercial practice which would target approximately 8.5 to 9% nickel content in standard 2209 type filler metal. The experimental electrodes were intended to obtain weld metal aimed at and below the low end of normal DSS weld metal ferrite specifications so that the CSCC resistance and the yield strength of the weld metal can be examined.

## 2 Experimental work

### 2.1 Material

The material purchased for this investigation is standard 22 Cr 5 Ni duplex stainless steel designated as UNS S32205, commonly known as 2205. Four cut plates with dimensions 1000 mm (L)  $\times$  150 (W)  $\times$  25 (T) were procured. The chemical composition as provided in the test certificate of Outokompu is shown in Table 1, with pitting resistance equivalent number (PRE<sub>N</sub>) calculated as Cr + 3.3Mo + 16 N = 35.7. Corrosion resistance according to EN ISO 3652-2C was reported as satisfactory after solution heat treatment at 1100 °C and quenched (forced air + water).

### 2.2 Welding filler metal

Three lots of rutile coated electrodes were donated by Ms. GEE Ltd., Kalyan (West) Thane Mumbai, India. Starting from a standard commercial AWS E2209-16 formulation, nickel was increased in the coating intended to achieve three targets of 9.5–10.5%, 10.5–11.5%, and 11.5–12.5% nickel, referred to herein after as A electrodes, B electrodes, and C electrodes, respectively, in a standard size of 3.15  $\times$  350 mm in length. Each lot of 10 kg wt. of varied nickel composition was tested for deposit composition by the manufacturer, with results given in Table 2. It is to be noted that only nickel content is varied

in all batches of electrodes, while the rest of the composition is as per E2209-16 standard composition.

It was expected that using these increased nickel electrodes, weld metal deposits would provide ferrite contents in the range of approximately 14 to 30%, or 20 to 40 FN, which levels are below the commonly specified range of 35 to 60% ferrite.

### 2.3 Welding procedure and test coupon preparation

Before welding was started, the electrodes were re-dried in an oven at a temperature of 300 °C for 2 h, then held at 150 °C per the manufacturer's recommendations. Figure 2 shows the weld test coupons of the 2205 DSS. No preheating was applied as per standard practice. Voltage and current were maintained within the ranges recommended by the electrode manufacturer, i.e., 18–22 V and 80–120 A respectively. Interpass temperature was measured for each pass using both digital thermometers and temperature indicating crayons to maintain 150 °C maximum in accordance with standard recommendations. The test pieces were welded in flat position. Welds were deposited with stringer bead technique at an average travel speed of 160–170 mm/min. Heat input, normally recommended to be in the range of 0.5–2.5 kJ/mm, averaged 0.73 kJ/mm. A backing strip of 2205 was used. The plates of the test piece were restrained in such a way that a sufficiently flat test piece is produced for extraction of specimens.

The dimensions of the test setup are as shown in Fig. 2a and Table 3, extracted from ISO 15792-1 *Welding consumables — Test methods — Part 1: Test methods for all-weld metal test specimens in steel, nickel and nickel alloys*. Figure 2b shows the actual joint, restrained by strong backs.

### 2.4 Chemical analysis

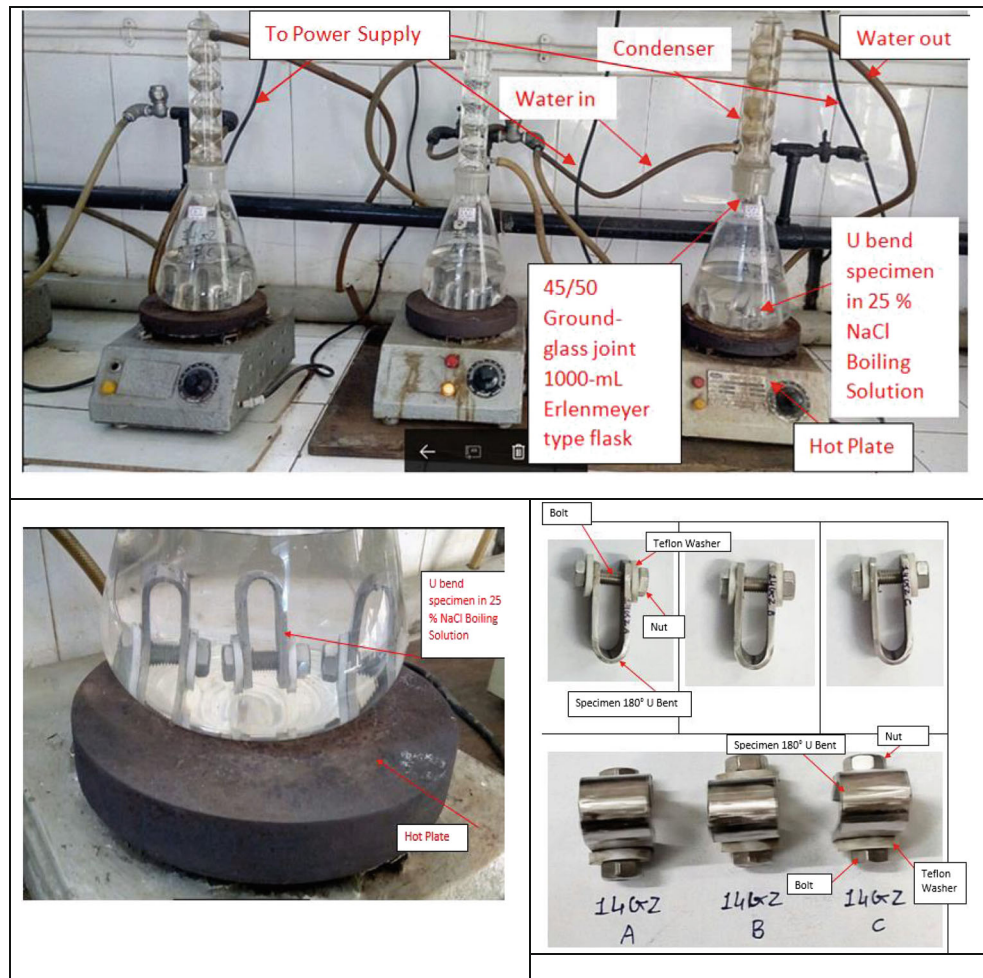
Chemical analysis of each weld joint sample was carried out by an optical emission spectrometer method as per ASTM E-1086-08 [17] with Spectramax X instrument on the weld centerline at the mid-thickness. The averages of the analyses at two spots for each weldment are reported in Table 4. It can be noted that the analyses reflect some dilution as compared with the analyses, especially for nickel, given in Table 2.

**Table 4** Chemical analysis of the weld metal centerline at the mid-thickness

Weldment identification	Composition, percent by weight									
	C	S	P	Mn	Si	Cr	Ni	Mo	Cu	N
A electrode weld sample	0.024	0.004	0.023	1.250	0.600	23.320	9.28	3.12	0.076	0.163
B electrode weld sample	0.022	0.004	0.024	1.120	0.580	23.340	9.73	3.11	0.076	0.150
C electrode weld sample	0.023	0.002	0.024	1.180	0.540	21.79	12.32	3.06	0.076	0.151



**Fig. 3** Set of specimens in prestressed “U” bend, three specimens per lot, immersed in boiling 25% NaCl solution in each flask on a hot plate equipped with condenser arrangement



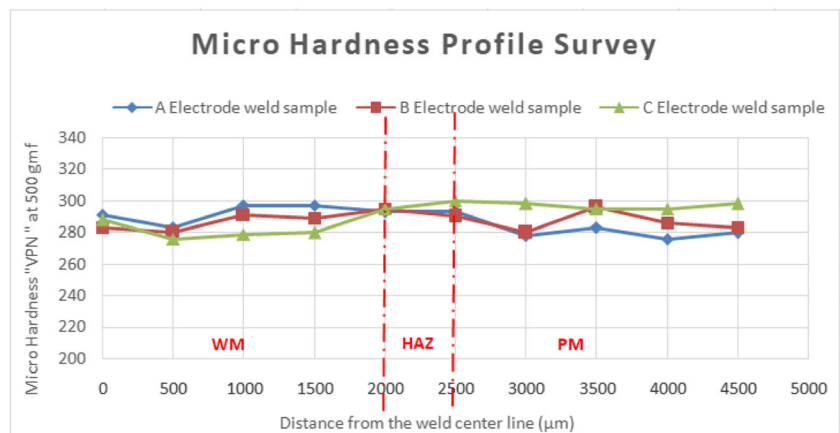
## 2.5 Ferrite measurement

### 2.5.1 Metallographic ferrite measurement

Measurement of ferrite was done with the point count method [18] and with Feritscope [19]. Preparation included

metallographic polishing to a 0.05  $\mu\text{m}$  finish, examined at  $\times 400$  magnification. A grid is then superimposed over the image and based on the counts of the number of points, which fall within the desired phase micro constituent. Statistical analysis reveals the fraction of points, which fall within the desired phase, and the volume fraction is then calculated.

**Fig. 4** Microhardness profile survey measured at 10 locations from weld centerline to base metal



**Table 5** Weld metal tensile test results

Weldment identification	Ferrite % using ASTM E562	Ferrite content at T/2 location using Ferriscope®	Tensile strength, MPa		Yield strength, MPa (at 0.2% proof load)		% elongation		% RA	
			Sample 1	Sample 2	Sample 1	Sample 2	Sample 1	Sample 2	Sample 1	Sample 2
AWS A5.4 [30]	N.S.	N.S.	690 min	N.S.	N.S.	20 min	N.S.			
ISO 3581[31]	N.S.	N.S.	550 min	450 min	450 min	20 min	N.S.			
E2209-16 <sup>1</sup>	N.S.	30–50	700 to 800	600 to 680	600 to 680	20 to 25	–			
A electrode weld sample	40.94%	31.7	853	860	687	25.7	684	25.3	46.5	46.3
B electrode weld sample	38.45%	28.2	858	852	678	24.6	683	26.0	51.0	48.7
C electrode weld sample	12.15%	14.0	760	778	588	27.4	644	28.0	64.6	63.0

<sup>1</sup> Typical results for a commercial product from the supplier of experimental electrodes  
N.S., not specified

## 2.5.2 Magnetic ferrite measurement with Feritscope

A Fischer Feritscope Model 2531 was calibrated on a standard set provided by Fischer and used for checking the ferrite number as well as ferrite percentage on a sample. Measurement of ferrite was taken on the transverse weld section at the mid-thickness on the centerline at three different points.

## 2.6 Hardness survey of test coupons

The microhardness of weld, HAZ, and base metal were determined as per ASTM E-384 [20] using the Vickers hardness tester. Specimens were measured for microhardness at ten different locations along the mid-thickness at 500 μm intervals with 500 g load according to the prescribed method in the standard.

## 2.7 Charpy V-notch impact test

One set (3 specimens) for V-notch Charpy impact test as per ASTM A 370-14 [21], AWS B4.0 [22] standard dimensions 10 mm × 10 mm × 55 mm were extracted from each weld coupon. The specimens were broken on 350 J impact testing machine at –40 °C test temperature.

## 2.8 Weld metal tensile test

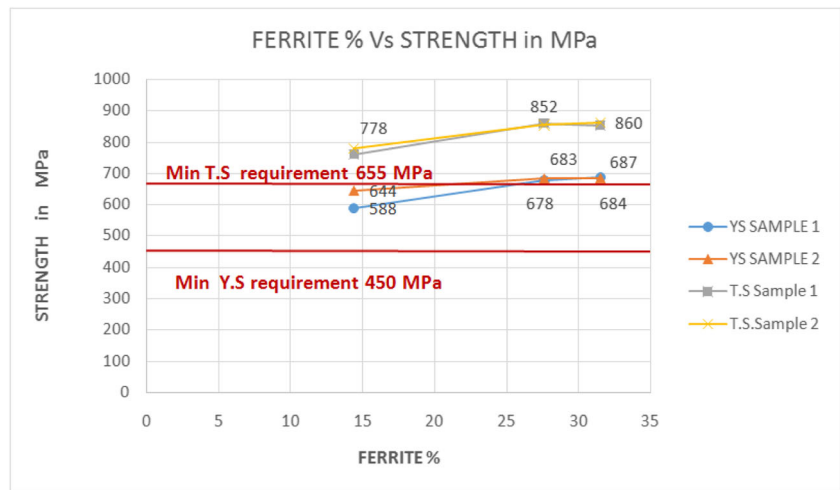
The all-weld tensile test as per ISO 15792-1:2000 [16] was employed to assess weld metal mechanical properties ultimate tensile strength (UTS), yield strength (YS), tensile elongation (% EL), and reduction of area (% RA). In this test, in the as-welded condition, two samples were extracted from each weld test coupon, longitudinal to the welding direction, with dimensions 12.5-mm diameter × 60-mm length with an initial gauge length of 50 mm and were loaded in a 40-ton universal testing machine to conduct the test.

## 2.9 Pitting corrosion test

In the present investigation, increasing the Ni content while leaving all other elements as in the standard E2209-16 composition has, from the point of view of this study, the benefit of reducing the ferrite content while leaving the pitting resistance index (PRE<sub>N</sub>) essentially unchanged, as per the pitting resistance equivalent (PRE<sub>N</sub>) formula:  $PRE_N = \%Cr + 3.3 \times \%Mo + 16 \times \%N$ .

The resistance to pitting and crevice corrosion increases with the content of chromium, molybdenum, and nitrogen content in the steel. But work by Potgieter et al. [14] suggests to investigate the effect of varied nickel content on the pitting corrosion resistance. Accordingly, specimens with dimensions 28.20 × 17.78 × 13.10 mm from each weld test coupon were extracted and exposed in 6% ferric chloride of 1.3-pH test

**Fig. 5** Tensile and yield strength as a function of % ferrite for 2205



solution environment maintained at 22 °C (± 2 °C) for 24 h as per ASTM G48 Method A [23].

**2.10 Chloride stress corrosion cracking (CSCC) test**

In the present research work, the standard “U-bend” stressed welded joint test samples for evaluating the CSCC resistance were extracted from the same weldments employed for carrying out various mechanical tests. The idea is to correlate the susceptibility to CSCC while ferrite content is being varied in the weld metal.

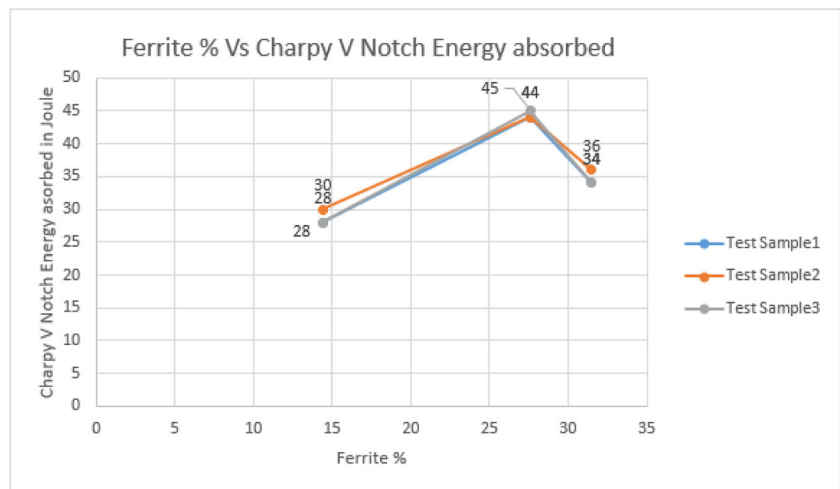
To meet the objectives of the research program, the ASTM G 123 [24] was used. Some standard DSS manufacturer’s data sheets [25] and NACE data [26–28] suggest that it is resistance to CSCC in boiling sodium chloride solution that should be evaluated, but not in magnesium chloride solution. Accordingly, ASTM Standard G 36 [29] was not employed in the present work. The ASTM G 123 test method employed

to evaluate CSCC resistance is stated in the standard to be suitable for wrought stainless steels, including duplex (ferritic-austenitic) stainless and an alloy with up to about 33% nickel. The method is stated to be suitable for the cast or welded conditions [24].

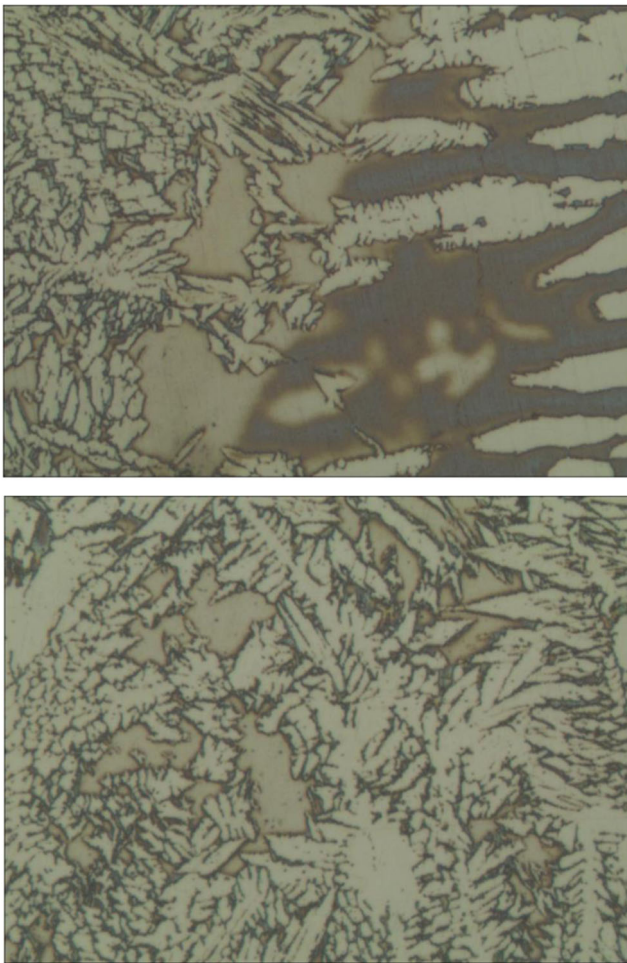
The methods of fabricating U-bend specimens are also provided in Practice G 30 but with a restriction in dimensions in such a way that sufficiently thick specimen (that should not rupture or crack under tightened condition) should pass through a 45/50 ground-glass joint 1000-mL Erlenmeyer type flask. The legs of the U-bends are sufficiently tightened to reach the plastic range (i.e., exceed the yield strength) with the bolt, nut, and flat washer of a material that is resistant to corrosion in the given test solution environment [24].

A standard size specimen as suggested in ASTM G 123 [24] was used, with dimensions 102 mm (L) × 19 mm (W) × 3.2 mm (T), with a hole at each end of 9.5 mm in diameter, and a center distance between the holes of 82.6 mm. The length of

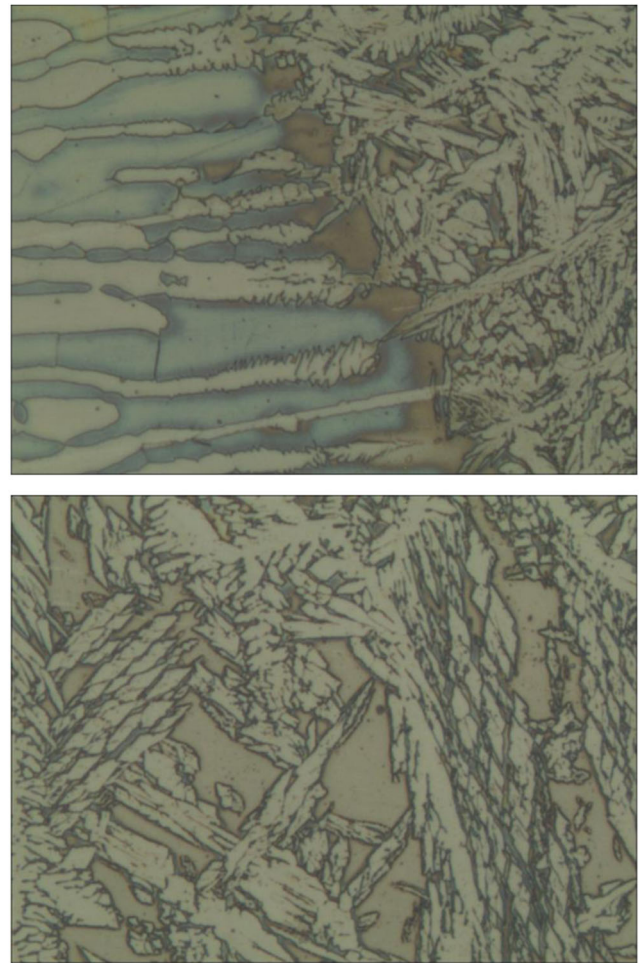
**Fig. 6** Charpy V-notch energy absorbed at – 40 °C for the experimental weld metals







**Fig. 7** Representative microstructures of the A electrode weld sample. Top: at the fusion boundary, base metal HAZ on the right and weld metal on the left, X400. Bottom: at the weld center, X400



**Fig. 8** Representative microstructures of the B electrode weld sample. Top: at the fusion boundary, base metal and HAZ on the left, weld metal on the right, X400. Bottom: at the weld center, X400

the specimen was transverse to the direction of the weld, with the weld at the center of the length, and the specimen was press bent to 180 degrees and then stressed with corrosion-resistant bolts, nuts, and washers as shown in Fig. 3.

The specimens were then degreased and cleaned with halogen-free solvent, rinsed, and dried as per standard guidelines. Before dipping into the solution, bent specimens were examined with  $\times 20$  magnification and no cracks were found. Three specimens were prepared from each weld test coupon and were subsequently placed in the flask containing the sodium chloride solution. Then the flask was placed on the hot plate with a fitted condenser and the test begun by boiling the solution at 106 to 110 °C.

After a week (approximately 168 h) exposure, the specimens were removed from the flask, rinsed, and dried, and examined under  $\times 20$  magnification. The test solution pH was also to be monitored. The solution was changed, and this process was repeated for up to 6 weeks (approximately 1000 h). Time to crack was recorded, as per ASTM G 123 [24].

### 3 Discussions of results

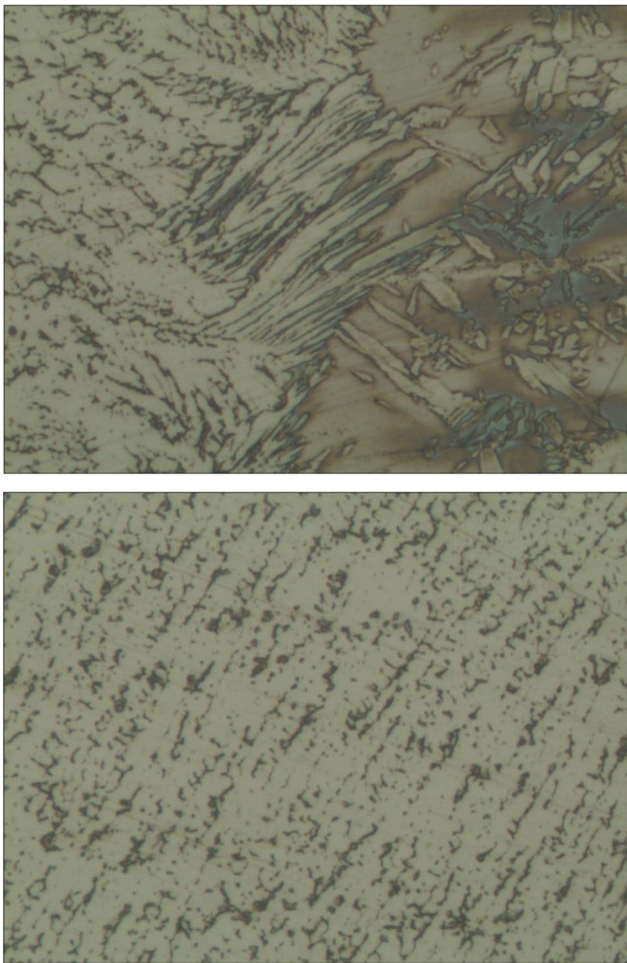
#### 3.1 Effect of ferrite content on the hardness profile

Figure 4 presents the hardness profiles (made at 500  $\mu\text{m}$  intervals) for the groove welds made with the three nickel levels. Measurements were made along the mid-thickness. It can be seen that there is not a major drop in hardness as the nickel content of the weld metal increases. Weld metal and HAZ hardness is quite similar to that of the 2205 base metal within the normal range of scatter.

#### 3.2 Effect of ferrite content on mechanical properties

Table 5 presents the filler metal classification standard requirements for AWS E2209-16 electrode deposits and for ISO 3581 E 22 9 3 N L electrode deposits. These requirements are followed by typical results for the commercial E2209-16 from the datasheet of the supplier of experimental electrodes. The





**Fig. 9** Representative microstructures of the C electrode weld sample. Top: at the fusion boundary, base metal and HAZ on the right, weld metal on the left, X400. Bottom: at the weld center, X400

actual longitudinal all-weld metal tensile test results for the experimental electrodes are also included in Table 5, along with Feritscope ferrite measurement averages on the weld centerline at the mid-thickness. It can be seen that the mechanical property requirements of the filler metal specifications are comfortably exceeded by the deposits of the experimental

electrodes at all nickel levels investigated, even at the lowest ferrite content.

Table 5 shows that the tensile and yield strengths are somewhat lower for the highest nickel electrode C, but the classification requirements are exceeded for all experimental electrodes. Moreover, the ASTM A240 standard for 2205 base metal requires 450 MPa yield strength minimum and 655 MPa tensile strength minimum. Figure 5 plots the tensile strength and yield strength results against ferrite content so that it is clear how large is the margin. So all-weld metal test results comfortably exceed those requirements as well as the filler metal specification requirements. It is to be noted that AWS A5.4 only requires tensile strength, not yield strength. It is also noteworthy that ISO 3581 requires yield strength for the 22 9 3 N L or 2209 filler metal to be 450 MPa minimum. All-weld metal and base metal requirements are exceeded.

Figure 6 depicts Charpy V-notch energy absorbed (joule) at  $-40\text{ }^{\circ}\text{C}$  as a function of ferrite content for the enriched nickel E2209-16 weld metals. While 27 J is exceeded in all cases, it is recognized that some fabrication specifications require as much as 47 J. In such cases, E2209-15 electrodes would normally be chosen instead of E2209-16 electrodes. It is well known that the highly basic slag system of E2209-15 electrodes produces weld metal of lower oxygen content than that of E2209-16 electrode deposits, resulting in higher absorbed Charpy V-notch energy for the former.

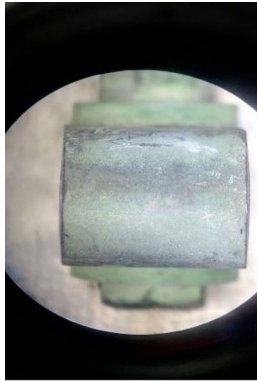
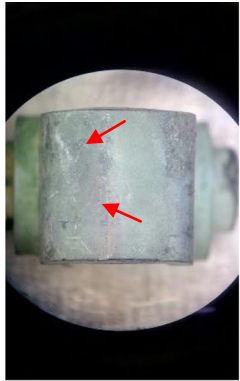

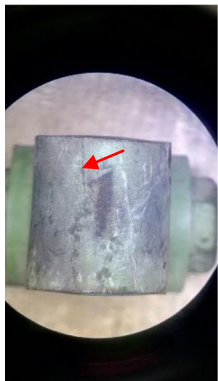
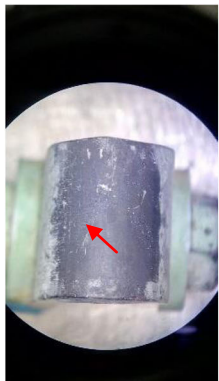
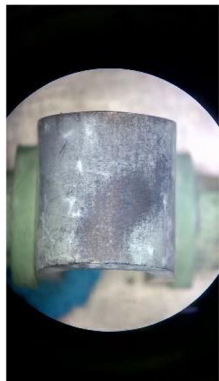

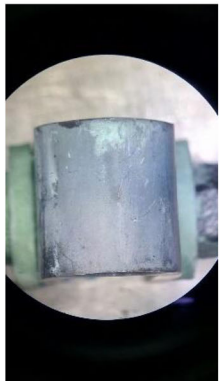
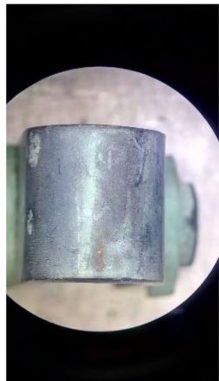
### 3.3 Microstructure examinations

Specimens of weld test coupons were polished and electrochemically etched in sodium hydroxide (40 g NaOH in 100 ml distilled water) for 5 s as per ASTM A 923, Method A [32]. The microstructure in all cases shows no significant presence of inter-metallic phases and precipitates. Microstructures at the fusion boundary (high dilution area) and in the weld metal center (low dilution area corresponding to the location of the tensile test specimens) are shown in Figs. 7, 8, and 9. The

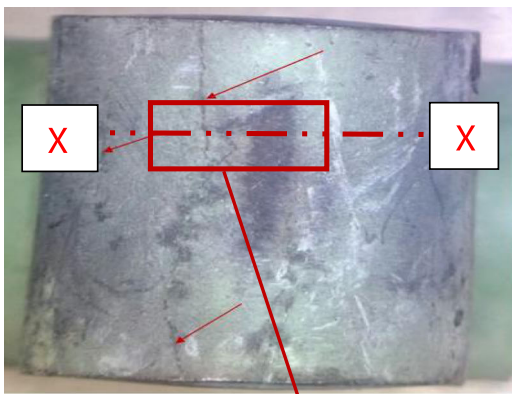
**Table 6** ASTM G48A pitting test results

Weld sample	A Electrode weld sample	B Electrode weld sample	C Electrode weld sample
Sample photo at 20 X magnification			
Weight loss, g	0.0003	0.0007	0.0007
Corrosion rate, g/m <sup>2</sup>	0.15	0.36	0.32

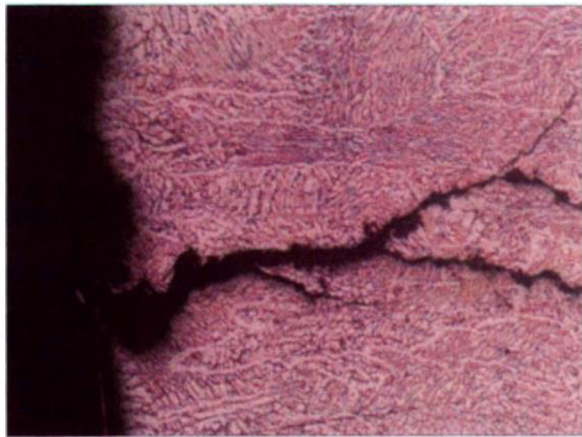
**Table 7** Periodic observation of CSSC samples at bend portion

Test coupon	Observations		
	Sample 1	Sample 2	Sample 3
<b>A Electrode weld samples</b>	No crack observed at bend portion at exposure of 1000 hrs.	Crack observed at bend portion after 3 weeks(21 days or 504 hours)	No crack observed at bend portion at exposure of 1000 hrs.
			
<b>B Electrode weld samples</b>	Crack observed at bend portion after 2 weeks (14 days or 366 hours)	Crack observed at bend portion after 2 weeks(14 days or 366 hours)	No crack observed at bend portion at exposure of 1000 hours.
			
<b>C Electrode weld samples</b>	No crack observed at bend portion after exposure of 1000 hrs.	No crack observed at bend portion after exposure of 1000 hrs.	No crack observed at bend portion after exposure of 1000 hrs.
			





**(a) – B Electrode weld CSCC sample 1 with crack found after 2 weeks exposure**

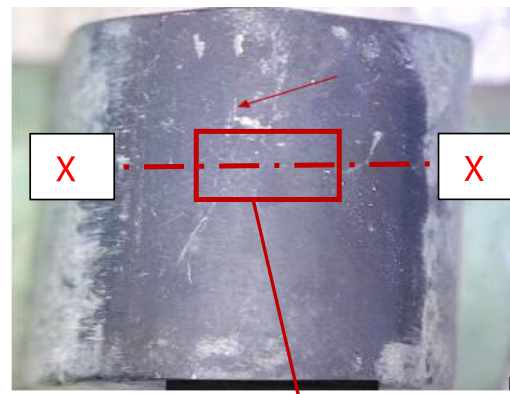


**(b) – B Electrode weld CSCC sample 1 cross section etched with 10 % ammonium persulfate (electrolytic), showing crack branching typical of CSCC**

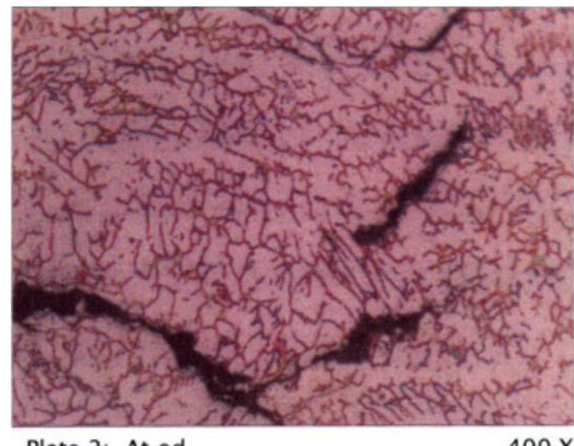
**Fig. 10** **a** B electrode weld CSCC sample 1 with crack found after 2 weeks exposure. **b** B electrode weld CSCC sample 1 cross section etched with 10% ammonium persulfate (electrolytic), showing crack branching typical of CSCC

ferrite phase is etched dark, while the austenite phase is etched light in all of these figures.

The microstructures of the A electrode weld sample and of the B electrode weld sample are very similar at the corresponding locations. There is no visible precipitation in the HAZ, but there is some over-etching in the ferrite areas of the HAZ which produces the dark tint. The weld metal near the fusion boundary and in the weld center has a typical duplex microstructure, reflecting solidification in the F-mode (essentially 100% ferrite solidification) and formation of



**(a) – B Electrode weld CSCC sample 2 with crack found after 2 weeks exposure**



**(b) – B Electrode weld CSCC sample 2 cross section etched with 10 % ammonium persulfate (electrolytic), showing crack branching typical of CSCC**

**Fig. 11** **a** B electrode weld CSCC sample 2 with crack found after 2-week exposure. **b** B electrode weld CSCC sample 2 cross section etched with 10% ammonium persulfate (electrolytic), showing crack branching typical of CSCC

austenite only in the solid state, as described by Lippold and Kotecki [5].

The microstructure of the C electrode weld sample is considerably different from that of the other two samples. There is some plate-like formation of austenite near the fusion boundary (indicating F-mode solidification). However, the remainder of the weld metal near the fusion boundary and at the weld center exhibits the skeletal ferrite typical of FA-mode solidification (primary ferrite with austenite appearing during the later stages of solidification), as described by Lippold and Kotecki [5].

### 3.4 Effect of ferrite content on pitting behavior

Pitting corrosion results as per ASTM G48 Method A, show very marginal loss of weight ranging from 0.0003 to 0.0007 g, or, in terms of weight loss per unit area, 0.15 to 0.32 g/m<sup>2</sup>. Samples were examined at  $\times 20$  magnification. No pitting was observed after 24 h of exposure in 6% FeCl<sub>3</sub> test solutions at 22 °C as shown in Table 6.

### 3.5 Effect of ferrite content on CSCC

Weekly, the specimens were removed from the test solution, washed, dried, and examined under  $\times 20$  magnification for cracks, and the test solution pH was measured. If cracks were found, the test was stopped for the cracked sample only. For uncracked specimens, the test solution was renewed and the exposure was repeated for another week until a total exposure of 6 weeks (approximately 1000 h) was accumulated, as recommended in ASTM G 123 [24]. Table 7 presents the test results, with arrows indicating the location of cracks. Table 7 shows only samples which exhibited cracks at some time in the exposure and samples which reached 1000 h exposure without cracking.

Cross sections covering the cracks were taken of the B electrode weld samples 1 and 2, which revealed cracks. The effort was to confirm whether the crack developed is “branched”, which would be typical of CSCC cracking. The samples were polished and etched using 10% ammonium persulfate (electrolytic) and were examined under an optical microscope at  $\times 100$ – $400$  magnification as shown in Figs. 10 and 11. Higher magnification photomicrographs of the crack cross sections seem to clearly establish that the cracks are CSCC. Figure 12 shows a bent sample after sectioning.

It is interesting to note that one of the three A electrode weld samples was cracked after 3-week exposure while the other two were uncracked after the full 1000-h exposure. Further, two of the three B electrode weld samples were cracked after 2-week exposure while the third was uncracked after the full 1000-h exposure. Finally, the three C electrode weld samples (lowest ferrite content) were uncracked after the full 1000-h exposure. This last result is quite unexpected, especially since the microstructure of the C electrode weld metal reflects FA solidification mode instead of F solidification mode.

Note that ASTM G 123 [24], Clause 12.1.3, indicates that there is maximum variability of results when materials of intermediate CSCC resistance are evaluated, so that cracking in one or two A electrode and B electrode samples is not entirely unexpected.



**(a) – B Electrode weld CSCC sample 2 sectioning**



**(b) - Perspective view of B Electrode weld CSCC sample 2 sectioning**

**Fig. 12** a B electrode weld CSCC sample 2 sectioning. b Perspective view of B electrode weld CSCC sample 2 sectioning

## 4 Conclusions

1. Yield strength and tensile strength requirements of base metal and filler metal classifications are exceeded at all ferrite levels investigated, even though the C electrode weld sample exhibited evidence of FA solidification mode (skeletal ferrite) instead of the F solidification mode typical of duplex stainless steel weld metal.
2. No pitting was observed in any of the test samples when tested at 22 °C in the ASTM G48 Method A test.
3. No CSCC was observed after 1000-h exposure in the C electrode weld samples with ferrite content of 14%.



4. Minimum ferrite requirements in fabrication specifications can be relaxed according to the findings of this study.

**Acknowledgments** Sincere thanks are extended to Mr. Umesh Agarwal, CEO, Ms. GEE Ltd., Kalyan (West) Thane Mumbai, India, for providing especially formulated SMAW electrodes, on complimentary basis, to achieve the objectives of this research program. Also, sincere thanks are extended to Mr. Fredrik Prabhu, Sr. Manager, ITW India Pvt. Ltd. for giving permission for utilizing welding equipment and for technical guidance and resource support by his welding engineer, Mr. Subhash Das, for arranging the resource facility of the weld test coupons preparation.

**Funding information** The authors would like to express their appreciation for financial support provided by GUJCOST-DST under Minor Research Project Scheme award of Research grant (2014-15.) Ref. GUJCOST Letter Dated 30th March 2015.

**Publisher's note** Springer Nature remains neutral with regard to jurisdictional claims in published maps and institutional affiliations.

## References

- Edition T (2015) Use of duplex stainless steels in the oil refining industry
- Messer B, Oprea V, Wright A (2007) Duplex stainless steel welding : best practices. In: Stainless steel world. KCI Publishing, Zutphen, pp 53–63
- (2001) Practical guidelines for the fabrication of duplex stainless steels, revised edition. International Molybdenum Association, USA
- Kotecki DJ (1986) Ferrite control in duplex stainless steel weld metal. *Weld J* 65(10):273–s–278-s American Welding Society, Miami
- Lippold JC, Kotecki DJ (2005) Welding metallurgy and weldability of stainless steels. Wiley, Hoboken, pp 234–262
- Gunn RN Duplex stainless steels microstructure, properties and applications. Woodhead Publishing Ltd, Abington
- Baesslack WA III, Duquette DJ, Savage WF (1978) Technical Note : Stress corrosion cracking in duplex stainless steel weldments. *Weld J* 57(6):175-s–177-s American Welding Society, Miami
- Van Gelder K, Erling JG, Damen JWM, Visser A (1987) The stress corrosion cracking of duplex stainless steel in H<sub>2</sub>S/CO<sub>2</sub>/Cl-environments. *Corros Sci* 27(10/11):1271–1279 Elsevier B.V., Amsterdam
- Krishnan KN, Rao KP (1991) Effect of microstructure on stress corrosion cracking behaviour of austenitic stainless steel weld metals. *Mater Sci Eng A* 142:79–85
- Liou H-Y, Hsieh R-I, Tsai W-T (2002) Microstructure and stress corrosion cracking in simulated heat-affected zones of duplex stainless steels. *Corros Sci* 44:2841–2856 Elsevier B.V., Amsterdam
- Raman RKS, Siew WH (2010) Role of nitrite addition in chloride stress corrosion cracking of a super duplex stainless steel. *Corros Sci* 52(1):113–117 Elsevier B.V., Amsterdam
- Al-Joboury AI, Mourad AHI, Alawar A, Zour MA, Abuzeid OA (2010) Stress corrosion cracking of stainless steels recommended for building brine recirculation pumps. *Eng Fail Anal* 17(6):1337–1344 Elsevier B.V., Amsterdam
- Yang J, Wang Q, Wei Z, Guan K (2014) Case Studies in Engineering Failure Analysis Weld failure analysis of 2205 duplex stainless steel nozzle. *Biochem Pharmacol* 2(2):69–75 Elsevier B.V., Amsterdam
- Potgieter JH, Olubambi PA, Cornish L, Machio CN, Sherif ESM (2008) Influence of nickel additions on the corrosion behaviour of low nitrogen 22% Cr series duplex stainless steels. *Corros Sci* 50(9):2572–2579 Elsevier B.V., Amsterdam
- Kotecki DJ, Siewert TA (1992) WRC-1992 constitution diagram for stainless steel weld metals : a modification of the WRC-1988 diagram. *Weld J* 71(5):171-s–178-s American Welding Society, Miami
- ISO 15792-1:2000(E) Welding consumables — Test methods — Part 1: Test methods for all-weld metal test specimens in steel, nickel and nickel alloys. International Organization for Standardization, Geneva
- ASTM E1086 Standard test method for optical emission vacuum spectrometric analysis of stainless steel by the point-to-plane excitation technique. ASTM International, West Conshohocken
- ASTM E562 Standard practice for determining volume fraction by systematic manual point count. ASTM International, West Conshohocken
- ASTM A800/A800M Standard Practice for Steel Casting, Austenitic Alloy, Estimating Ferrite Content Thereof. ASTM International, West Conshohocken
- ASTM E384 Standard Test Method for Microindentation Hardness of Materials. ASTM International, West Conshohocken
- ASTM A370 Standard Test Methods and Definitions for Mechanical Testing of Steel Products. ASTM international, West Conshohocken
- (2016) AWS B4.0 Standard Methods for Mechanical Testing of Welds, 8th edn. American Welding Society, Miami
- ASTM G48 Standard practices for pitting and crevice corrosion resistance of stainless steel and related alloy by use of ferric chloride solution. ASTM international, West Conshohocken
- ASTM G 123 Standard Test Method for Evaluating Stress-Corrosion Cracking of Stainless Alloys with Different Nickel Content in Boiling Acidified Sodium Chloride Solution. ASTM International, West Conshohocken
- (2013) Outokumpu duplex stainless steel data sheet. Outokumpu Oyj, Helsinki
- Stress Corrosion Cracking Properties of UNS S32101 – A new Duplex Stainless Steel with low Nickel Content, page 1–16, 2–2007, Outokumpu Oyj, Helsinki
- The welding consequences of replacing austenitic with duplex stainless steel, 1–2009, Outokumpu Oyj, Helsinki
- Duplex stainless steels in the hydrometallurgical industry, pp 2-16, 1-2010, and Corrosion testing of stainless steel for metal leaching applications, pp 7–18, 1–10, Outokumpu Oyj, Helsinki
- ASTM G 36 Standard practice for evaluating stress-corrosion cracking resistance of metals and alloys in a boiling magnesium chloride solution. ASTM International, West Conshohocken
- AWS A5.4/A5.4M Specification for stainless steel electrodes for shielded metal arc welding. American Welding Society, Miami
- ISO 3581 Welding consumables – covered electrodes for manual metal arc welding of stainless and heat-resisting steels – classification. International Organization for Standardization, Geneva
- ASTM A 923 Standard practices for detecting Intermetallic phases in Duplex Austenitic/ Ferritic stainless steel. ASTM International, West Conshohocken